Thermodynamic Properties of Ligand Binding by Monoclonal Anti-fluorescyl Antibodies†

James N. Herron, David M. Kranz,‡ David M. Jameson,§ and Edward W. Voss, Jr.*

Department of Bioengineering, University of Utah, Salt Lake City, Utah 84112

Received January 17, 1986; Revised Manuscript Received April 14, 1986

ABSTRACT: The effects of temperature on the binding of fluorescein by three monoclonal anti-fluorescyl antibodies (4-4-20, 20-19-1, and 20-20-3) were assessed by measurements of affinity constants (K_a) over a temperature range of 2–70 °C. Values for K_a were determined from the degree of ligand association by using fluorescence methodology. Curvilinear van't Hoff plots (ln K_a vs. T^{-1}) were observed for all three antibodies, indicating that their standard enthalpy changes ($\Delta H°$) were temperature dependent. This phenomenon was further investigated by plotting the changes in unitary free energy (ΔG_u), standard enthalpy ($\Delta H°$), and unitary entropy (ΔS_u) vs. temperature. Strong temperature dependencies were observed for enthalpy and entropy values, while free energy plots were only weakly dependent on temperature. At low temperatures (4 °C), entropy played a major role in the binding of fluorescein by all three antibodies, while enthalpy dominated at higher temperatures. This was a consequence of the negative heat capacity changes ($\Delta C_p° \approx -320$ cal K^{-1} mol^{-1}) observed for these antibodies, which produced a negative trend in both enthalpy and entropy values with increasing temperature. The negative heat capacity values also indicated that the hydrophobic effect was instrumental in the binding of fluorescein. Entropy changes were lower than expected for hydrophobic binding alone, suggesting that other forces were acting to mitigate the hydrophobic effect. One possibility was that the binding of fluorescein acted to restrain vibrational fluctuations in the active-site region, producing negative changes in both heat capacity and entropy. Sturtevant (1977) developed an analytic method for evaluating both the hydrophobic and vibrational contributions to binding. When Sturtevant's procedure was applied to anti-fluorescyl antibodies, unfavorable vibrational contributions were observed for all three antibodies. The effect was most pronounced with the 20-20-3 protein, and the least with the 4-4-20 protein. Considering that 4-4-20 exhibited the highest affinity of the three proteins, it is possible that one mechanism of generating high-affinity active sites may involve structural changes in the active site which reduce the size of the unfavorable vibrational contribution. The effects of pressure on the binding of fluorescein by anti-fluorescyl antibodies were assessed by measurements of affinity constants (K_a) over a pressure range of 10^{-3}–3 kbar. Standard volume changes ($\Delta V°$) were determined at 25 °C from ΔG_u vs. pressure plots. Positive $\Delta V°$ values were observed for 4-4-20 and 20-20-3, while 20-19-1 exhibited a negative volume change. It was not clear from the pressure plots why the standard volume change of the 20-19-1 protein was opposite in sign to the other two antibodies. In keeping with our hydrophobic and vibrational analysis of thermodynamic parameters, we analyzed standard volume changes in terms of hydrophobic and vibrational components. All three antibodies exhibited positive ($\sim$90 mL mol^{-1}) contributions from the hydrophobic effect and negative contributions ($\sim$−80 mL mol^{-1}) from vibrational effects. This result was analogous to the relative hydrophobic and vibrational contributions observed for thermodynamic parameters and indicative of hapten-induced conformational changes in the antigen binding region.

The immune system is capable of producing specific antibodies to an almost unlimited number of antigenic determinants. Recent advances in immunogenetics have defined a number of different genetic mechanisms responsible for the diversity of antibody active sites (Leder, 1982; Gearhart, 1983, 1984; Reilly et al., 1984; Rudikoff et al., 1984), but the exact molecular basis of antigenic specificity remains largely unexplored. Several three-dimensional structures of complexes of antigen binding fragments with ligands have been reported, including vitamin K_1OH with New, a λ,IgG1 protein of human origin (Amzel et al., 1974), and phosphorylcholine with McPC 603, a κ,IgA protein of murine origin (Segal et al., 1974; Padlan, 1977). At least one Bence-Jones light chain dimer (Mcg) binds ligands in the crystalline state. Its main binding cavity is shaped like a truncated cone and is lined with 21 amino acid side chains, 12 of which are aromatic. Therefore, it has provided a good model for the binding of aliphatic and aromatic ligands (Edmundson et al., 1974, 1984). Binding studies of New, McPC 603, and Mcg have helped define the molecular basis of low-affinity interactions, but new studies of specific antibodies of medium and high affinities are needed to broaden our understanding of antigenic specificity.

The advent of hybridoma technology has enabled the production of monoclonal antibodies of specific immune origin. The genetics and solution binding properties of several monoclonal anti-hapten systems have been described in recent years including anti-carbohydrate (Rudikoff et al., 1983;

† This work was supported by Grant AI 20960, awarded by the National Institutes of Health, Department of Health and Human Services. J.N.H. is a postdoctoral fellow supported by Grant PDF 8166016, awarded by the National Science Foundation, and Grant GM 08843, National Research Service Award from the National Institutes of Health.

* Address correspondence to this author at the Department of Microbiology, University of Illinois at Urbana–Champaign, Urbana, IL 61801.

‡ Present address: Center for Cancer Research, Massachusetts Institute of Technology, Cambridge, MA 02139.

§ Present address: Department of Pharmacology, University of Texas Health Science Center at Dallas, Dallas, TX 75235.

0006-2960/86/0425-4602$01.50/0

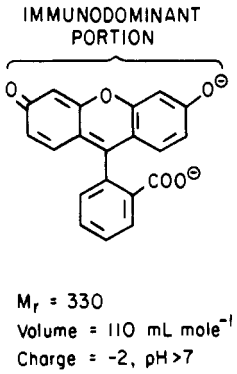

M_r = 330
Volume = 110 mL mole^{-1}
Charge = -2, pH>7

FIGURE 1: Structural formula of fluorescein. For elicitation of antibodies, fluorescein 5-isothiocyanate was covalently conjugated to a carrier protien (keyhole limpet hemocyanin). Fluorescein absorbed strongly in the visible spectrum, exhibiting a molar extinction coefficient of 73 000 M^{-1} cm^{-1} at 493 nm. Fluorescence emission occurred at 515 nm with a quantum efficiency of 92%. Upon binding to anti-fluorescyl antibodies, the absorption maximum of fluorescein was shifted 10–15 nm to the red, and its fluorescence was quenched by ≥95%.

Perlmutter et al., 1984), anti-arsonate (Slaughter et al., 1982; Margolies et al., 1983; Rothstein & Gefter, 1983), anti-dinitrophenyl (Scott & Fleischman, 1982), and anti-fluorescein (Kranz & Voss, 1981a,b, 1983; Kranz et al., 1982, 1983). The abundance and homogeneity of these antibodies offer a unique opportunity to pursue correlated studies of their genetics, thermodynamics, and three-dimensional structures. Such correlations will ultimately lead to a firmer understanding of the molecular basis of the humoral immune response.

The anti-fluorescein system is ideal for studies of structure and function because it offers both a wide range of binding affinities (10^5–10^{10} M^{-1}) and a variety of experimental techniques for measuring affinities, kinetics, and thermodynamics (Kranz & Voss, 1981a; Kranz et al., 1982; Herron, 1984). Moreover, fluorescein is a site-filling antigenic group (Voss et al., 1976) which eliminates anomalous binding effects arising from heterogeneous linkages of the hapten to the carrier protein (Karush, 1978). Additionally, anti-fluorescyl antibodies exhibit little or no cross-reactivity for rhodamine compounds (Voss et al., 1976; Kranz & Voss, 1981a), suggesting that the xanthonyl ring is the immunodominant portion of the fluorescein molecule (see Figure 1). The antigen binding affinities, reaction kinetics, and spectral properties of several different monoclonal anti-fluorescyl antibodies were characterized in previous studies (Kranz et al., 1982). Interestingly, these antibodies differed greatly in affinity, binding mechanism, and spectral properties, but all followed a common two-step association reaction. The first step was the bimolecular association of ligand and antibodiy, followed by a slower conformational transition which probably resulted from the conformational "fine-tuning" of active-site residues to better accommodate the ligand. This two-step mechanism is thought to be a generally operative mechanism in antigen–antibody reactions [see review by Pecht (1982)].

In this paper, we describe the thermodynamic characterization of three anti-fluorescyl antibodies (4-4-20, 20-19-1, and 20-20-3). We have attempted to correlate these data with previous kinetic studies (Kranz et al., 1982) in order to understand the thermodynamic basis of hapten-induced conformational changes. From a thermodynamic perspective, there are two forces competing in these antibodies. First is the hydrophobic effect (Tanford, 1980), which provides the thermodynamic driving force for fluorescein binding. However, the binding of fluorescence also restricts the mobility of active-site residues, which makes an unfavorable contribution to the standard free energy of binding. We believe that this second effect forms the basis for the hapten-induced conformational changes.

Experimental Procedures

Production and Purification of Hybridoma Proteins. Anti-fluorescyl antibody-secreting cell lines (4-4-20, 20-19-1, and 20-20-3) were generated by fusion of BALB/c splenic lymphocytes with the Sp 2/0-Ag 14 myeloma cell line, as described by Kranz and Voss (1981). Spleen cells were removed from the mouse on the fourth day following a secondary immunization with fluorescein 5-isothiocyanate, covalently conjugated to keyhole limpet hemocyanin (KLH). Hybridoma cells (ca. 5×10^6) were injected into BALB/c mice primed with pristane (2,6,10,14-tetramethylpentanedecane), and ascites fluids were collected 10–15 days after injection. Lipoproteins were removed from ascites fluid by sodium dextran sulfate precipitation (Kranz & Voss, 1984). γ-Globulin fractions were precipitated with 50%-saturated ammonium sulfate. Anti-fluorescyl antibodies were isolated from the γ-globulin fraction by affinity chromatography over Sepharose 6B conjugated to 5-aminofluorescein and eluted with 0.1 M fluorescein (Kranz & Voss, 1984). Excess fluorescein was removed by anion-exchange chromatography using Dowex 1-X8.

Temperature Perturbation Studies. Association constants (K_a) were determined from the degree of ligand association, using fluorescence intensity data as described by Li et al. (1976a,b). Fluorescence measurements were taken with an Aminco-Bowman (4-8202-SPF) spectrophotofluorometer. Samples were excited at 485 nm, and emission was measured through a Corning 3-69 cutoff filter (50% transmission at 525 nm). Solutions were buffered with 0.05 M potassium phosphate (pH 8), which maintained constant pH over the temperature range of the experiment. The temperature of the cuvette chamber was controlled with a constant-temperature water bath (Forma). A thermistor probe was placed in the cuvette chamber, which was connected to a direct-reading thermometer (YSI 8400). Analog signals from the fluorometer and thermometer were used to plot fluorescence intensity vs. temperature on an X-Y plotter (Hewlett-Packard).

In a typical experiment, temperature was elevated from 2 to 70 °C in increments of 1 °C. Fluorometer readings were allowed to settle after each temperature increment, allowing the solutions of equilibrate. A preliminary experiment was performed to establish the effects of temperature on the maximum fluorescence quenching constant (Q_{max}) of each monoclonal antibody. In this experiment, the concentration of unbound antibody was poised high enough to ensure that >99.9% of the fluorescence was bound. Under these conditions, the degree of ligand association was insensitive to small changes in affinity (less than 10-fold), and changes observed in fluorescence intensity are directly attributable to changes in Q_{max}. The experiment was then repeated at a lower antibody concentration, and affinity constants were computed at each temperature increment. Standard free energy ($\Delta G°$), standard enthalpy ($\Delta H°$), and standard entropy ($\Delta S°$) changes were determined from affinity (K_a) vs. temperature data by using the equations:

$$\Delta G° = -RT \ln K_a \quad (1)$$

$$\Delta H° = RT^2(\partial \ln K_a/\partial T)_P \quad (2)$$

$$\Delta S° = (\Delta H° - \Delta G°)/T \quad (3)$$

where R is the gas constant and T is the absolute temperature (kelvin). The derivative of ln K_a with respect to temperature

was determined by using Savitzky–Golay algorithms for least-squares numerical differentiation (Savitzky & Golay, 1964; Steiner et al., 1972).

In reactions involving different numbers of reactant and product species (e.g., hapten binding to antibodies), the magnitude of the free energy change is dependent on the concentration units chosen for the standard state. This effect is purely statistical in nature, resulting from the entropy of mixing. In early studies by Gurney (1953), the standard entropy change ($\Delta S°$) was defined as the sum of two components:

$$\Delta S° = \Delta S_u + R \ln \chi_M \quad (4)$$

where ΔS_u is the unitary contribution to entropy and is independent of the concentration units chosen for the standard state. The second term ($R \ln \chi_M$) is the cratic contribution to entropy, where χ_M is the mole fraction of a molecule at a concentration of 1.0 M. Because the concentration of water in dilute aqueous solution is 55.6 M, the cratic contribution to entropy is $R \ln (1/55.6)$ or -7.98 cal K^{-1} mol^{-1} (Kauzmann, 1959). Unitary free energy (ΔG_u) and unitary entropy (ΔS_u) values were determined from $\Delta G°$ and $\Delta S°$ values by using the equations:

$$\Delta S_u = \Delta S° - R \ln \chi_M = \Delta S° + 7.98 \quad (5)$$

$$\Delta G_u = \Delta G° - 7.98T \quad (6)$$

Thermodynamic parameters were analyzed by plotting ΔG_u, $\Delta H°$, and $-T\Delta S_u$ vs. temperature. Such plots illustrate the compensating effects of enthalpy and entropy on the free energy of binding, because $\Delta H°$ and $-T\Delta S_u$ possess the same sign and units (Szewczuk & Mukkur, 1977a,b; Mukkur, 1978, 1980). Heat capacity values ($\Delta C_p°$) were determined by linear regression of enthalpy vs. temperature plots, in accordance with the relation:

$$\Delta C_p° = (\partial \Delta H° / \partial T)_P \quad (7)$$

Hydrophobic and Vibrational Components of Thermodynamic Parameters. The hydrophobic effect has been implicated in a number of different protein–ligand interactions, as evidenced by their large, negative $\Delta C_p°$ values (Sturtevant, 1977). However, many of these reactions exhibited ΔS_u values much lower than expected for purely hydrophobic binding. Sturtevant (1977) proposed that the binding of ligand decreased the vibrational mobility of the protein, resulting in an unfavorable contribution to entropy. He developed an empirical method for analyzing the relative contributions of both intramolecular vibrations and the hydrophobic effect to protein–ligand thermodynamics. Vibrational (vib) components were computed as follows:

$$\Delta C_p°(\text{vib}) = [0.26\Delta C_p°(\text{thermo}) + \Delta S_u(\text{thermo})]/1.31 \quad (8)$$

$$\Delta S_u(\text{vib}) = 1.05\Delta C_p°(\text{vib}) \quad (9)$$

$$\Delta H°(\text{vib}) = 0.53T\Delta C_p°(\text{vib}) \quad (10)$$

$$\Delta G_u(\text{vib}) = -0.52T\Delta C_p°(\text{vib}) \quad (11)$$

where $\Delta C_p°$(thermo) and ΔS_u(thermo) were empirical values for heat capacity and unitary entropy changes, determined for anti-fluorescyl antibodies at 25 °C. Hydrophobic components were determined by subtraction of vibrational components from empirical values [e.g., ΔG_u(hydro) = ΔG_u(thermo) − ΔG_u(vib)].

Pressure Perturbation Studies. Sample solutions were compressed with the high-pressure apparatus described by Paladini and Weber (1981). Solutions were buffered with 0.05 M tris(hydroxymethyl)aminomethane hydrochloride (Tris-HCl) (pH 8), which was relatively insensitive to pressure changes. Fluorescence measurements were obtained with a fluorescence polarization instrument (Jameson et al., 1978) equipped with Ortec photon-counting electronics. Pressure bomb temperature was regulated at 20 ± 1 °C with a Lauda RC3 thermostatic bath. A standard protocol was followed in all pressure experiments: pressure was increased in increments of ca. 200 bar through a range of 10^{-3}–3 kbar. Fluorometer readings were allowed to settle for 10–20 min before measurements were recorded. The excitation shutter was closed during this period to minimize photobleaching. Sample preparations were maintained at maximum pressure for 60 min to test for long-term effects. Pressure was removed in 200–300-bar increments with 10–20-min settling times to assess the reversibility of pressure effects. Values for the maximum quenching constant (Q_{max}) and the affinity constant (K_a) were determined at each pressure increment by simultaneous measurement of fluorescence intensity and polarization, using a method described by Herron (1984). Polarization values were measured with the instrument in the "L" format. At elevated pressures, changes in the birefringency of the pressure bomb windows resulted in apparent depolarization. Birefringency corrections were determined by measuring fluorescence polarization at elevated pressures and −10 °C for a 10^{-6} M solution of fluorescein in concentrated glycerol. Window scrambling factors were computed as suggested by Paladini and Weber (1981). Fluorescein fluorescence was excited at 485 nm and emission monitored through a Corning 3-69 cutoff filter. Standard volume changes ($\Delta V°$) were determined by using the equation:

$$\Delta V° = (\partial \Delta G_u / \partial P)_T \quad (12)$$

Results and Discussion

Enthalpy–Entropy Compensation. Temperature data were initially analyzed by using van't Hoff plots (Figure 2). The curvilinear plots indicated that the enthalpies of these antibodies were temperature dependent. This result was not surprising, because the enthalpies ($\Delta H°$) and entropies (ΔS_u) of most reactions involving proteins exhibit strong temperature dependencies (Sturtevant, 1977). A phenomenon known as enthalpy–entropy compensation has been reported for polyclonal antibodies of both anti-dinitrophenyl (anti-Dnp) and anti-bovine serum albumin (anti-BSA) specificities (Szewczuk & Mukkur, 1977a,b; Mukkur, 1978, 1980; van Oss et al., 1982). These researchers observed a compensating effect in the contributions of enthalpy and entropy to free energy, which resulted in free energy (ΔG_u) being almost temperature independent. Compensation plots for 4-4-20, 20-19-1, and 20-20-3 are presented in Figure 3. Values for ΔG_u, $\Delta H°$, and $-T\Delta S_u$ are plotted vs. temperature, and the values of thermodynamic parameters at four different temperatures (4, 25, 37, and 50 °C) are listed in Table I. All three monoclonal anti-fluorescyl antibodies exhibited strong enthalpy–entropy compensation, while free energy values showed only a weak temperature effect.

Enthalpy–entropy compensation has a firm basis in thermodynamics. The temperature derivatives of both $\Delta H°$ and ΔS_u are functions of heat capacity ($\Delta C_p°$):

$$(\partial \Delta H° / \partial T)_P = \Delta C_p° \quad (13)$$

$$(\partial \Delta S_u / \partial T)_P = \Delta C_p° / T \quad (14)$$

Therefore, the slopes of both the $\Delta H°$ and $-T\Delta S_u$ vs. tem-

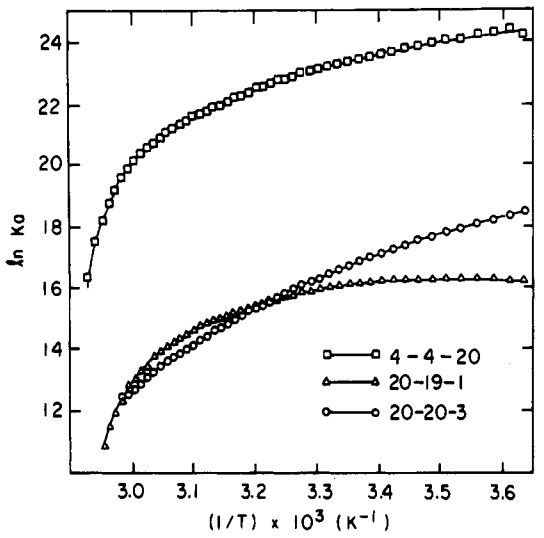

FIGURE 2: van't Hoff plots for monoclonal anti-fluorescyl antibodies (4-4-20, 20-19-1, and 20-20-3). The logarithm of the affinity constant (ln K_a) was plotted vs. reciprocal temperature ($1/T$) over a range of 275–343 K (2–70 °C). Values for K_a were determined by using fluorescence methodology (see Experimental Procedures). Fluorescein was excited at 485 nm, and emission was measured through a Corning 3-69 cutoff filter (50% transmission at 525 nm). (□) 4-4-20 IgG antibody (2.2 nM) and fluorescein (4.7 nM). (Δ) 20-19-1 IgG antibody (168 nM) and fluorescence (43 nM). (○) 20-20-3 IgG antibody (43 nM) and fluorescein (13 nM). Solutions were buffered with 0.05 M potassium phosphate (pH 8).

Table I: Temperature Dependence of Thermodynamic Parameters[a]

	thermodynamic parameters			
temp (°C)	ΔG_u (kcal mol^{-1})	$\Delta H°$ (kcal mol^{-1})	ΔS_u (cal K^{-1} mol^{-1})	$\Delta C_p°$ (cal K^{-1} mol^{-1})
4	−15.6	−6.6	32.4	−97
25	−16.2	−8.4	26.1	−266
37	−16.4	−13.9	8.2	−535
50	−16.4	−21.9	−17.1	−832
		20-19-1		
4	−11.2	2.0	47.8	−303
25	−11.9	−5.2	22.4	−330
37	−12.0	−11.1	3.0	−598
50	−11.9	−22.0	−31.3	−1503
		20-20-3		
4	−12.3	−8.7	12.9	−358
25	−12.3	−15.7	−11.4	−358
37	−12.1	−20.2	−26.2	−395
50	−11.6	−25.2	−42.1	−606

[a] Unitary free energy changes (ΔG_u) were determined directly from fluorescence data. van't Hoff enthalpy changes ($\Delta H°$) were determined by numerical differentiation of ln K_a vs. temperature data. Unitary entropy changes (ΔS_u) were calculated from ΔG_u and $\Delta H°$ values. Heat capacity changes ($\Delta C_p°$) were determined by numerical differentiation of $\Delta H°$ vs. temperature data.

perature plots are directly proportional to $\Delta C_p°$. Because both derivatives have the same sign, their contributions to the temperature derivative of free energy cancel out. Consequently, the temperature dependence of ΔG_u is given by

$$(\partial \Delta G_u/\partial T)_P = -\Delta S_u \qquad (15)$$

Typically, the magnitude of ΔS_u is less than 1% of ΔG_u, so the temperature dependency of ΔG_u is almost negligible.

Thermodynamic Driving Forces. Sturtevant (1977) described several possible sources of entropy and heat capacity changes in biochemical reactions: (1) the hydrophobic effect; (2) changes in intramolecular vibration; (3) changes in hydrogen bonding; (4) changes in exposure to electrostatic charges; and (5) temperature-dependent equilibria. Of these, the hydrophobic effect and changes in intramolecular vibration were considered the most important. Presumably, changes in electrostatic interactions and hydrogen bonding made only minor contributions to ΔS_u and $\Delta C_p°$, because the extent of solvent exposure to electrostatic charges and also the extent of hydrogen bonding were not expected to change significantly between the free and bound states. Temperature-dependent equilibria between two or more conformational states can contribute to heat capacity, resulting in values of $\Delta C_p°$ which are temperature dependent (Hearn et al., 1971). This phenomenon was probably operative in anti-fluorescyl antibodies at high temperatures (≥50 °C) and will be discussed more thoroughly below. The hydrophobic effect will be considered first.

(*1*) *The Hydrophobic Effect.* Aqueous solutions of aliphatic and aromatic molecules have positive heat capacities (Tanford, 1980). Thus, the binding of fluorescein should be accompanied by a negative change in heat capacity, which results from reduced solvent exposure of both the aromatic fluorescein molecule and apolar groups in the active site. Heat capacity changes of −266, −330, and −358 cal K^{-1} mol^{-1} were observed at 25 °C for 4-4-20, 20-19-1, and 20-20-3, respectively (Table I), indicating that the hydrophobic effect was instrumental in the binding of fluorescein by all three monoclonal antibodies.

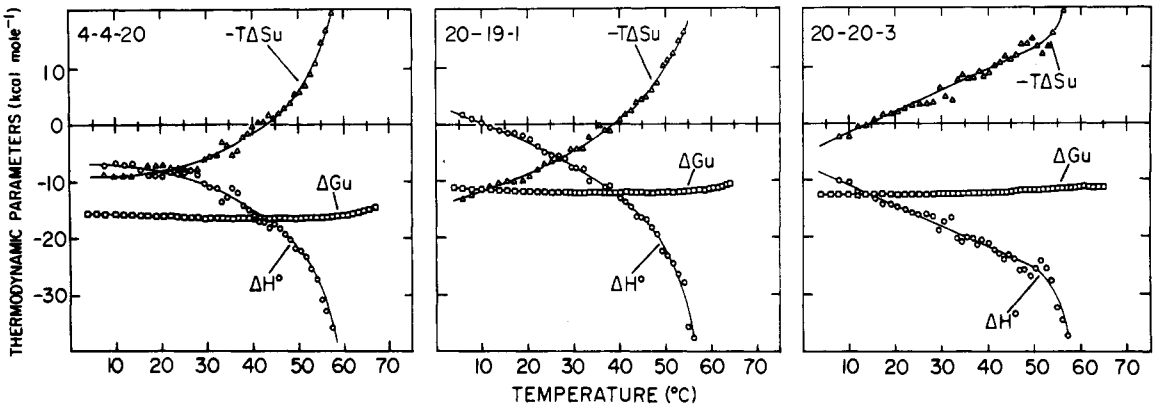

FIGURE 3: Enthalpy–entropy compensation plots. Thermodynamic parameters [ΔG_u (□), $\Delta H°$ (○), and $-T\Delta S_u$ (Δ)] for the binding of fluorescein by monoclonal anti-fluorescyl antibodies (4-4-20, 20-19-1, and 20-20-3) were plotted vs. temperature over a range of 2–70 °C. These plots illustrated the compensating effects of enthalpy ($\Delta H°$) and entropy (ΔS_u) on the free energy (ΔG_u) of binding, because $\Delta H°$ and $-T\Delta S_u$ possessed the same sign and units. Unitary free energy (ΔG_u) and unitary entropy (ΔS_u) values were used because they were independent of the concentration units chosen for the standard state. Values for thermodynamic parameters were computed as described under Experimental Procedures. Experimental conditions were the same as those listed in Figure 2.

Table II: Hydrophobic and Vibrational Contributions to Thermodynamic Parameters[a]

	hydrophobic components				vibrational components			
clone	ΔG_u (kcal mol^{-1})	$\Delta H°$ (kcal mol^{-1})	ΔS_u (cal K^{-1} mol^{-1})	$\Delta C_p°$ (cal K^{-1} mol^{-1})	ΔG_u (kcal mol^{-1})	$\Delta H°$ (kcal mol^{-1})	ΔS_u (cal K^{-1} mol^{-1})	$\Delta C_p°$ (cal K^{-1} mol^{-1})
4-4-20	−21.3	−3.2	60.6	−233	5.1	−5.2	−34.5	−32.9
20-19-1	−19.4	2.4	73.2	−282	7.5	−7.6	−50.8	−48.4
20-20-3	−24.7	−3.1	72.3	−278	12.4	−12.6	−83.8	−79.8

[a] Hydrophobic and vibrational contributions to the binding of fluorescein by anti-fluorescyl antibodies were determined by using an empirical method described by Sturtevant (1977). All values were determined at 25 °C, using thermodynamic data listed in Table I.

These values were similar to values of −100 to −300 cal K^{-1} mol^{-1} reported for the binding of dinitrophenyl (Dnp) ligands to monoclonal IgA immunoglobulins (MOPC 315 and 460) of murine plasmacytoma origin (Johnston et al., 1974). In fact, in a compendium of the thermodynamic properties of 12 different protein–ligand interactions, Sturtevant (1977) found that 11 of these reactions exhibited negative heat capacity changes in a range of −100 to −750 cal K^{-1} mol^{-1}. The sole exception was the binding of Dnp by polyclonal IgG antibodies of rabbit and bovine origin [see review by Mukkur (1980)]. Positive $\Delta C_p°$ values in a range of 300–500 cal K^{-1} mol^{-1} were reported by Mukkur and colleagues.

Entropy is generally considered to be the primary driving force of the hydrophobic effect at room temperature. Sturtevant (1977) found that the change in unitary entropy for the transfer of hydrocarbon compounds from nonpolar to aqueous media was nearly a constant fraction (−0.263 ± 0.046, at 25 °C) of the change in heat capacity. Unitary entropy changes of 26.1, 22.4, and −11.4 cal K^{-1} mol^{-1} were observed at 25 °C for 4-4-20, 20-19-1, and 20-20-3, respectively (Table I). All three values were significantly lower than $-0.263\Delta C_p°$, indicating that other forces were acting to mitigate the hydrophobic effect. Anomalously low entropy changes were observed for several other protein–ligand interactions, including avidin–biotin (Suurkuusk & Wadso, 1972), lipase–colipase (Donner et al., 1976), NAD^+ binding to glyceraldehyde-3-phosphate dehydrogenase (GPDH) (Niekamp et al., 1977), isoleucine binding to tRNA ligase (Hinz et al., 1976), and dinitrophenyllysine binding to MOPC-315 and MOPC-460 (Johnston et al., 1974).

(*2*) *Compensation of the Hydrophobic Effect by Intramolecular Vibrations.* Sturtevant (1977) attributed anomalously low entropy changes to ligand-induced changes in intramolecular vibrations. The heat capacities of most proteins containing large contributions from "soft" internal vibrational modes, which were weak enough to be perturbed by ligand binding. Sturtevant analyzed thermodynamic data obtained for two different protein–ligand interactions (NAD^+ binding to GPDH and isoleucine binding to tRNA ligase) in terms of vibrational and hydrophobic components. In both cases, the binding of ligand limited the vibrational flexibility of the protein, producing negative changes in both heat capacity and entropy. Thus, the favorable entropy changes produced by the hydrophobic effect were offset by unfavorable contributions from vibrational effects, leading to anomalously low entropy changes for the overall reaction.

Sturtevant's analysis was used to determine the hydrophobic and vibrational contributions to the binding of fluorescein by anti-fluorescyl antibodies, at 25 °C. The results of this analysis are listed in Table II. These data indicate that the hydrophobic effect provided the thermodynamic driving force for the binding of fluorescein but was partially offset by an unfavorable vibrational contribution. The magnitude of this compensation effect was greatest in the 20-20-3 protein and least in the 4-4-20 protein. Considering that 4-4-20 exhibited the highest affinity of the three proteins, it is possible that one mechanism for generating high-affinity active sites may involve structural changes in the active site which reduce the size of the unfavorable vibrational contribution.

(*3*) *Structural Nature of Vibrational Changes.* Sturtevant's proposal that intramolecular vibrations were the source of anomalously low entropy values may be too narrow in its scope. A considerable body of experimental evidence suggested that proteins are dynamic structures which constantly undergo conformational fluctuations [see review by Careri et al. (1979)]. These fluctuations include vibrational motions of the polypeptide backbone and amino acid side chains as proposed by Sturtevant, proton transfer reactions of ionizable side chains, vibrations of bound water molecules, conformational equilibria, and repositioning of subunits in oligomeric proteins. The damping of any of these fluctuations will make negative contributions to both entropy and heat capacity changes. In the case of anti-fluorescyl antibodies, we believe that the binding of fluorescein acts to reduce conformational fluctuations in the active-site region.

Hapten-induced conformational changes have been directly observed by kinetic studies of several different anti-hapten systems, including anti-fluorescein (Kranz et al., 1982). In a review of the subject, Pecht (1982) concluded that hapten-induced conformational changes were probably a generally operative mechanism in antibodies, although the biological significance of such changes was unknown. In three-dimensional studies of the binding of fluorescein and rhodamine to the Mcg Bence-Jones dimer, hapten-induced changes were observed in side chains, and to a lesser extent in the polypeptide backbone, which produced a "conformational tuning" of the Mcg active site to improve the complementarity with its ligand (Edmundson et al., 1984).

(*4*) *Aromatic–Aromatic Interactions.* Recent studies suggested that the pairing of aromatic side chains was instrumental in stabilizing protein structure (Burley & Petsko, 1985). Aromatic pairing is thought to result from attractive dispersion forces and coulombic interactions and exhibit ΔG_u values of −3 to −4 kcal mol^{-1}. Burley and Petsko analyzed the three-dimensional structure of neighboring aromatic groups in 34 proteins and observed that rings were separated by 4.5–7 Å, with dihedral angles between 30° and 90°. Aromatic pairing was also implicated in the binding of fluorescein and rhodamine to the Mcg Bence-Jones dimer (Edmundson et al., 1984). In fact, aromatic–aromatic interactions between side chains and fluorescent haptens in the binding cavity of the Mcg dimer exhibited intermolecular distances and dihedral angles almost identical with those observed by Burley and Petsko. On the basis of these observations, we speculate that aromatic–aromatic interactions were important in the binding of fluorescein by anti-fluorescyl antibodies. This hypothesis was consistent with observed thermodynamic data, because the pairing of aromatic molecules in an aqueous environment should exhibit positive changes in entropy and negative changes in heat capacity. In this respect, aromatic–aromatic inter-

actions can be regarded as a special case of the hydrophobic effect.

(5) *Temperature-Induced Conformational Changes.* Sturtevant (1977) observed that the heat capacity changes of most protein–ligand interactions were temperature independent in the vicinity of 25 °C. This trend was also observed for two of the anti-fluorescyl antibodies (20-19-1 and 20-20-3), as evidenced by their linear $\Delta H°$ vs. temperature plots, over a range of 2–40 °C (see Figure 3). In contrast, the heat capacity of 4-4-20 protein varied continuously with temperature. This phenomenon was observed previously for the association of proteolytic fragments of ribonuclease A and was attributed to temperature-induced conformational transitions (Hearn et al., 1971).

All three anti-fluorescyl antibodies exhibited temperature-dependent $\Delta C_p°$ values at temperatures ≥50 °C (Figure 3). In addition, significant decreases in affinity constants (K_a) were also observed at these temperatures (Figure 2). We believe that both effects were a prelude to thermal denaturation, which occurred at temperatures ≥70 °C (see below). Initial stages of denaturation probably involved a general relaxation of active-site conformation, including disruption of side-chain interactions and increased flexibility of the hypervariable loops, followed by the dissociation of the variable domains. In heavy and light chain reassociation studies, Watt and Voss (1979) found that the presence of fluorescein was instrumental in reestablishing the active-site conformation, once the variable domains had reassociated. Likewise, the presence of fluorescein could help reestablish the conformational of a disrupted active site. This process would proceed with large, negative changes in both heat capacity and entropy, because denatured (or partially denatured) proteins have much higher entropies and heat capacities than native proteins (Sturtevant, 1977).

Thermal Denaturation. As mentioned above, the affinities of all three antibodies decreased rapidly at temperatures ≥50 °C (see Figure 2). This trend was reversible to temperatures of ca. 65 °C but became irreversible at higher temperatures. The loss of reversibility was due to time-dependent thermal denaturation, which proceeded over a time course of about 30 min. It was not clear whether unliganded antibodies exhibited the same degree of temperature susceptibility as liganded antibodies, because thermal denaturation was inferred indirectly by the loss of fluorescein binding activity.

Pressure Perturbation Studies. Pressure perturbation data for the three anti-fluorescyl antibodies are shown in Figure 4, and values for standard volume changes of 5.1, −11.8, and 27.1 mL mol^{-1} were observed for 4-4-20, 20-19-1, and 20-20-3, respectively. The 4-4-20 protein was of particular interest. Its pressure plot was biphasic, with the transition point at 1.5 kbar. This phenomenon was also observed for the binding of fluorescent ligands to the Mcg Bence-Jones dimer and was attributed to pressure-induced conformational changes (Herron et al., 1985). The high-pressure form of the 4-4-20 protein exhibited a volume change of 19.8 mL mol^{-1}. The hydrophobic effect was expected to make significant contributions to standard volume changes. The transfer of hydrocarbon compounds from nonpolar to aqueous media is characterized by volume changes of ca. −20 mL mol^{-1} (Edsall & Gutfreund, 1983) and heat capacity changes of ca. 60 cal K^{-1} mol^{-1} (Sturtevant, 1977). Therefore, the hydrophobic contribution to the standard volume change can be estimated as follows:

$$\Delta V°(\text{hydro}) \simeq -0.333\Delta C_p°(\text{hydro}) \qquad (16)$$

Using this relation, $\Delta V°$(hydro) values of 78, 94, and 93 mL mol^{-1} were calculated for the 4-4-20, 20-19-1, and 20-20-3 proteins, respectively. These values were significantly greater

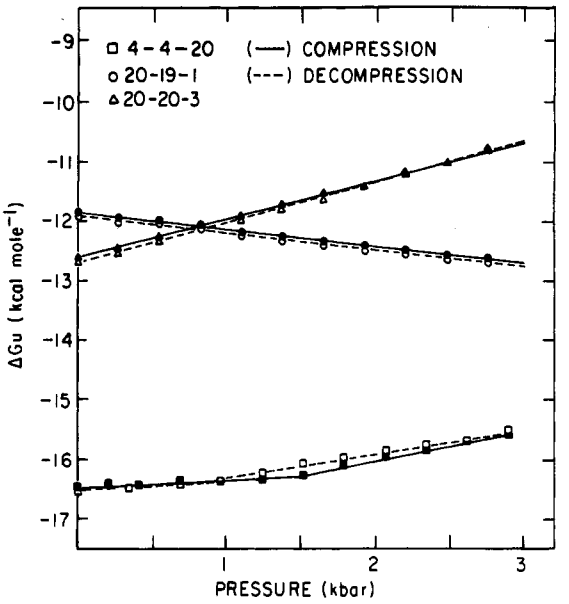

FIGURE 4: Standard volume changes ($\Delta V°$) for the binding of fluorescein by monoclonal anti-fluorescyl antibodies determined by plotting unitary free energy (ΔG_u) vs. pressure over a range of 10^{-3}–3 kbar. Values for ΔG_u were determined by using fluorescence methodology (see Experimental Procedures). Fluorescein was excited at 485 nm, and emission was measured through a Corning 3-69 cutoff filter (50% transmission at 525 nm). (□) 4-4-20 IgG antibody (4.9 nM) and fluorescein (10.3 nM). (○) 20-19-1 IgG antibody (54 nM) and fluorescein (85 nM). (△) 20-20-3 IgG antibody (48 nM) and fluorescein (110 nM). Solutions were buffered with 0.05 M Tris-HCl (pH 8), which was relatively insensitive to pressure changes. Plots are shown for both compression (—) and decompression (---). Standard volume changes ($\Delta V°$) of 5.1, −11.8, and 27.1 mL mol^{-1} were observed for 4-4-20, 20-19-1, and 20-20-3, respectively.

than the experimentally determined $\Delta V°$ values, indicating that other forces were acting to mitigate the hydrophobic contributions.

One possibility was that the binding of fluorescein acted to restrain vibrational fluctuations in the active-site region, producing a negative contribution to the standard volume change. Potential volume changes in proteins occur mainly by rotation around torsion angles, because bond distances and angles are not altered at pressures lower than 12 kbar (Benson & Drickamer, 1957). Torgerson et al. (1979) classified binding sites as "hard" and "soft". A hard site is typically formed from contiguous regions of polypeptide chain that have very limited torsional flexibility. A soft site is usually produced by polypeptide segments from different subunits or from different parts of the same chain. A hard site cannot decrease its volume with increasing pressure and exhibits a positive standard volume change, while a soft site can be compressed and exhibits a negative standard volume change.

By these critera, antibody active sites are soft sites and should exhibit negative volume changes. Assuming that the standard volume change was the sum of hydrophobic and vibrational components, then the vibrational contribution [$\Delta V°$(vib)] can be determined as follows:

$$\Delta V°(\text{vib}) = \Delta V° - \Delta V°(\text{hydro}) \qquad (17)$$

With this equation, $\Delta V°$(vib) values of −73, −106, and −66 mL mol^{-1} were calculated for 4-4-20, 20-19-1, and 20-20-3, respectively. Although these were only rough estimates, they did suggest that all three antibodies possessed soft sites and that the binding of fluorescein produced significant conformational changes.

Conclusions. These studies have shown that the hydrophobic effect was the primary thermodynamic driving force

behind the binding of fluorescein by anti-fluorescyl antibodies. Hydrogen bonding and electrostatic interactions are generally thought to be of equal magnitude in both solution and active site and have little or no thermodynamic impact (Tanford, 1962). However, this does not lessen their importance in establishing the stringent stereospecificity of the active site. In three-dimensional studies of the binding of aromatic haptens by the Mcg Bence-Jones dimer, aromatic–aromatic interactions were primarily responsible for stereospecificity, although both hydrogen bonds and electrostatic interactions were involved to a lesser extent (Edmundson et al., 1984).

We propose that the presence of hapten is necessary to orient active-site residues into their optimum conformation for binding. In the vacant active site, side-chain atoms can freely fluctuate in the volume occupied by the hapten. Upon binding, fluctuations are more restrained, leading to the negative contributions to entropy and heat capacity changes that Sturtevant (1977) attributed to vibrational effects. Indeed, this hapten-induced "tightening" of active-site conformation may form the structural basis for the hapten-induced conformational changes which have been observed in kinetic studies of anti-fluorescein (Kranz et al., 1982) and several other anti-hapten systems [see review by Pecht (1982)].

Registry No. Fluorescein, 2321-07-5.

REFERENCES

Amzel, L. M., Poljak, R. J., Saul, F., Varga, J. M., & Richards, F. F. (1974) *Proc. Natl. Acad. Sci. U.S.A. 71*, 1427.

Benson, A. M., & Drickamer, H. G. (1957) *J. Chem. Phys. 27*, 1164.

Burley, S. K., & Petsko, G. A. (1985) *Science (Washington, D.C.) 229*, 23.

Careri, G., Fasella, P., & Gratton, E. (1979) *Annu. Rev. Biophys. Bioeng. 8*, 69.

Donner, J., Spink, C. H., Borgstrom, B., & Sjoholm, I. (1976) *Biochemistry 15*, 5413.

Edmundson, A. B., Ely, K. R., Girling, R. L., Abola, E. E., Schiffer, M., Westholm, F. A., Fausch, M. D., & Deutsch, H. F. (1974) *Biochemistry 13*, 3816.

Edmundson, A. B., Ely, K. R., & Herron, J. N. (1984) *Mol. Immunol. 21*, 561.

Edsall, J. T., & Gutfreund, H. (1983) *Biothermodynamics*, p 154, Wiley, New York.

Gearhart, P. J. (1983) *Ann. N.Y. Acad. Sci. 418*, 171.

Gearhart, P. J. (1984) *Ann. Immunol. (Paris) 135C*, 137.

Gefter, M. L. (1983) *Ann. N.Y. Acad. Sci. 418*, 48.

Gurney, R. W. (1953) *Ionic Processes in Solution*, p 89, McGraw-Hill, New York.

Hearn, R. P., Richards, F. M., Sturtevant, J. M., & Watt, G. D. (1971) *Biochemistry 10*, 806.

Herron, J. N. (1984) in *Fluorescein Hapten: An Immunological Probe* (Voss, E. W., Jr., Ed.) p 49, CRC Press, Boca Raton, FL.

Herron, J. N., Ely, K. R., & Edmundson, A. B. (1985) *Biochemistry 24*, 3453.

Hinz, H. J., Weber, K., Flossdorf, J., & Kula, M. R. (1976) *Eur. J. Biochem. 71*, 437.

Jameson, D. M., Weber, G., Spencer, R. D., & Mitchell, G. (1978) *Rev. Sci. Instrum. 49*, 510.

Johnston, M. F. M., Barisas, B. G., & Sturtevant, J. M. (1974) *Biochemistry 13*, 390.

Karush, F. (1978) in *Immunoglobulins* (Litman, G. W., & Good, R. A., Eds.) p 85, Plenum Press, New York.

Kauzmann, W. (1959) *Adv. Protein Chem. 14*, 1.

Kranz, D. M., & Voss, E. W., Jr. (1981a) *Mol. Immunol. 18*, 889.

Kranz, D. M., & Voss, E. W., Jr. (1981b) *Proc. Natl. Acad. Sci. U.S.A. 78*, 5807.

Kranz, D. M., & Voss, E. W., Jr. (1983) *Mol. Immunol. 20*, 1301.

Kranz, D. M., & Voss, E. W., Jr. (1984) in *Fluorescein Hapten: An Immunological Probe* (Voss, E. W., Jr., Ed.) p 15, CRC Press, Boca Raton, FL.

Kranz, D. M., Herron, J. N., & Voss, E. W., Jr. (1982) *J. Biol. Chem. 257*, 6987.

Kranz, D. M., Ballard, D. W., & Voss, E. W., Jr. (1983) *Mol. Immunol. 20*, 1313.

Leder, P. (1982) *Sci. Am. 246*, 102.

Li, T. M., Hook, J. W., Drickamer, H. G., & Weber, G. (1976a) *Biochemistry 15*, 3205.

Li, T. M., Hook, J. W., III, Drickamer, H. G., & Weber, G. (1976b) *Biochemistry 15*, 5571.

Margolies, M. N., Juszczak, E. C., Near, R., Marshak-Rothstein, A., Rothstein, T. L., Sato, V. L., Siekevitz, M., Smith, J., Wysocki, L. J., & Gefter, M. L. (1983) *Mol. Immunol. 20*, 161.

Mukkur, T. K. S. (1978) *Biochem. J. 172*, 39.

Mukkur, T. K. S. (1980) *Trends Biochem. Sci. (Pers. Ed.) 5*, 72.

Niekamp, C. W., Sturtevant, J. M., & Velick, S. F. (1977) *Biochemistry 16*, 436.

Padlan, E. A. (1977) *Q. Rev. Biophys. 10*, 35.

Paladini, A. A., & Weber, G. (1981) *Rev. Sci. Instrum. 52*, 419.

Pecht, I. (1982) in *The Antigens VI* (Sela, M., Ed.) p 1, Academic Press, New York.

Perlmutter, R. M., Crews, S. T., Klotz, J., Livant, D., Siu, J., & Hood, L. (1984) *Ann. Immunol. (Paris) 135C*, 83.

Reilly, E. B., Bloberg, B., Imanishi-Kari, T., Tonegana, S., & Eisen, H. N. (1984) *Proc. Natl. Acad. Sci. U.S.A. 81*, 2484.

Rudikoff, S., Pawlita, M., Pumphery, J., Mushinsky, E., & Potter, M. (1983) *J. Exp. Med. 158*, 1385.

Rudikoff, S., Pawlita, M., Pumphery, J., & Heller, M. (1984) *Proc. Natl. Acad. Sci. U.S.A. 81*, 2162.

Savitzky, A., & Golay, M. J. E. (1964) *Anal. Chem. 36*, 1627.

Scott, M. G., & Fleischman, J. B. (1982) *J. Immunol. 128*, 2622.

Segal, D. M., Padlan, E. A., Cohen, G. H., Rudikoff, S., Potter, M., & Davies, D. R. (1974) *Proc. Natl. Acad. Sci. U.S.A. 71*, 4298.

Slaughter, C. A., Siegelman, M.., Estess, P., Barasoain, I., Nisonoff, A., & Capra, J. D. (1982) in *Development Immunology: Clinical Problems and Aging*, p 45, Academic Press, New York.

Steiner, J., Termonia, Y., & Deltour, J. (1972) *Anal. Chem. 44*, 1906.

Sturtevant, J. M. (1977) *Proc. Natl. Acad. Sci. U.S.A. 74*, 2236.

Suurkuusk, J., & Wadso, I. (1972) *Eur. J. Biochem. 28*, 438.

Szewczuk, M. R., & Mukkur, T. K. S. (1977a) *Immunology 32*, 111.

Szewczuk, M. R., & Mukkur, T. K. S. (1977b) *Immunology 33*, 11.

Tanford, C. (1962) *J. Am. Chem. Soc. 84*, 4240.

Tanford, C. (1980) *The Hydrophobic Effect*, 2nd ed., Wiley, New York.

Torgerson, P. M., Drickamer, H. G., & Weber, G. (1979) *Biochemistry 18*, 3079.
van Oss, C. J., Absolom, D. R., & Bronson, P. M. (1982) *Immunol. Commun. 11*, 139.
Voss, E. W., Jr., Eschenfeld, W., & Root, R. T. (1976) *Immunochemistry 13*, 447.
Watt, R. M., & Voss, E. W., Jr. (1979) *J. Biol. Chem. 254*, 7105.

Electron Paramagnetic Resonance Properties of the S_2 State of the Oxygen-Evolving Complex of Photosystem II

J.-L. Zimmermann* and A. W. Rutherford‡

Service de Biophysique, Département de Biologie, Centre d'Etudes Nucléaires de Saclay, 91191 Gif-sur-Yvette Cedex, France

Received February 5, 1986; Revised Manuscript Received April 2, 1986

ABSTRACT: Electron paramagnetic resonance (EPR) signals arising from components in photosystem II have been studied in membranes isolated from spinach chloroplasts. A broad EPR signal at $g = 4.1$ can be photoinduced by a single laser flash at room temperature. When a series of flashes is given, the amplitude of the $g = 4.1$ signal oscillates with a period of 4, showing maxima on the first and fifth flashes. Similar oscillations occur in the amplitude of a multiline signal centered at $g \simeq 2$. Such an oscillation pattern is characteristic of the S_2 charge accumulation state in the oxygen-evolving complex. Accordingly, both EPR signals are attributed to the S_2 state. Earlier data from which the $g = 4.1$ signal was attributed to a component different from the S_2 state [Zimmermann, J.-L., & Rutherford, A. W. (1984) *Biochim. Biophys. Acta 767*, 160–167; Casey, J. L., & Sauer, K. (1984) *Biochim. Biophys. Acta 767*, 21–28] are explained by the effects of cryoprotectants and solvents, which are shown to inhibit the formation of the $g = 4.1$ signal under some conditions. The $g = 4.1$ signal is less stable than the multiline signal when both signals are generated together at low temperature. This indicates that the two signals arise from different populations of centers. The differences in structure responsible for the two different EPR signals are probably minor since both kinds of centers are functional in cyclic charge accumulation and seem to be interconvertible. The difference between the two EPR signals, which arise from the same redox state of the same component (a mixed-valence manganese cluster), is proposed to be due to a spin-state change, where the $g = 4.1$ signal reflects an $S = {}^3/_2$ state and the multiline signal an $S = {}^1/_2$ state within the framework of the model of de Paula and Brudvig [de Paula, J. C., & Brudvig, G. W. (1985) *J. Am. Chem. Soc. 107*, 2643–2648]. The spin-state change induced by cryoprotectants is compared to that seen in the iron protein of nitrogenase.

The evolution of oxygen due to the photooxidation of water by higher plants, green algae, and cyanobacteria occurs by a four-step mechanism (Joliot et al., 1969). The experimental data are interpreted in a model which envisages five states, S_0, S_1, S_2, S_3, and S_4, of the oxygen-evolving complex (Kok et al., 1971). These states represent successive oxidation states, each generated by a single turnover of the photosystem II (PS II)[1] reaction center. In the model, S_0 and S_1 are stable in the dark, while S_2 and S_3 can deactivate back to S_1. S_4 reacts rapidly to S_0 in a millisecond and O_2 is evolved.

An EPR signal centered at $g = 2$ and having 19–20 hyperfine lines has been observed in broken chloroplasts following excitation with a single flash (Dismukes & Siderer, 1980). This multiline signal has been seen in thylakoids frozen under illumination (Hansson & Andréasson, 1982) or following illumination at 200 K (Brudvig et al., 1983). It has also been seen in PS II particles under the same conditions. This signal has been shown to originate from the S_2 state of the oxygen-evolving system (Dismukes & Siderer, 1980; Hansson & Andréasson, 1982; Brudvig et al., 1983; Zimmermann & Rutherford, 1984). The best evidence for this assignment is that, following a series of flashes, its amplitude oscillates with a period of 4, having maxima on the first and fifth flashes (Dismukes & Siderer, 1980; Zimmermann & Rutherford, 1984; Franzén et al., 1985). It has been suggested that this signal arises from an $S = {}^1/_2$ state of a manganese cluster (Dismukes & Siderer, 1980; Hansson & Andréasson, 1982; Brudvig et al., 1983; Dismukes et al., 1982; Andréasson et al., 1983; Hansson et al., 1984). A recent study, however, has shown that the saturation behavior and temperature dependence of this signal depend both on the length of dark adaptation before illumination and on the illumination temperature (de Paula & Brudvig, 1985; Beck et al., 1985). The multiline signal was shown to be best interpreted as originating from the interaction of an $S_1 = {}^1/_2$ state of a manganese cluster with an $S_2 = 1$ system (de Paula & Brudvig, 1985). This model also predicted the existence of an $S = {}^3/_2$ ground state.

An EPR signal at $g = 4.1$ was discovered recently, which was also attributed to a donor side component (Casey & Sauer, 1984; Zimmermann & Rutherford, 1984). It was suggested that this component was an intermediate carrier between the

‡Supported by the CNRS.

[1] Abbreviations: DCMU, 3-(3,4-dichlorophenyl)-1,1-dimethylurea; Me_2SO, dimethyl sulfoxide; EDTA, ethylenediaminetetraacetic acid (sodium salt); EPR, electron paramagnetic resonance; MES, 4-morpholineethanesulfonic acid; PPBQ, phenyl-*p*-benzoquinone; PS II, photosystem II; Q_A, primary quinone acceptor; Q_B, secondary quinone acceptor; S_i, charge accumulation states of the O_2-evolving complex; Chl, chlorophyll.

0006-2960/86/0425-4609$01.50/0